

Energy Balances and Uniaxial Failure of Solid Propellants

A. H. LEPIE and A. ADICOFF, *Chemistry Division (Code 3858), Research Department, Naval Weapons Center, China Lake, California 93555*

Synopsis

A simple test procedure was used to determine the total damage in a propellant that accumulates during a tensile test from 0% strain to failure. Damage energies of two propellants were measured at various temperatures and straining rates, and Williams-Landel-Ferry shift procedures were applied to the results. The reduced master curves for the total damage energy at failure are used to compare the failure behavior of the two propellants.

INTRODUCTION

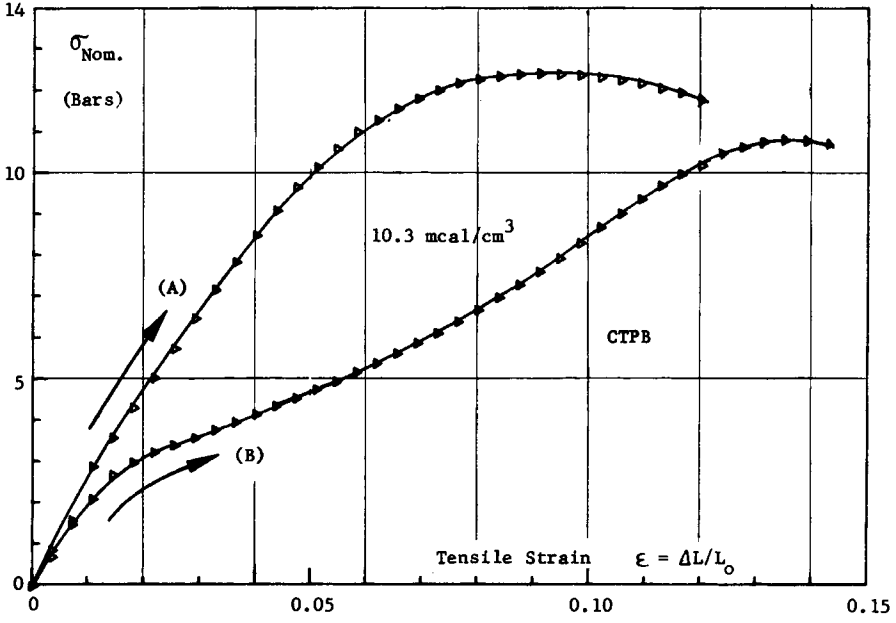
The failure behavior and cumulative damage properties of rubbers and solid propellants have been studied from different viewpoints by several investigators. Smith^{1,2} describes the ultimate failure properties of rubbers by a failure envelope of log stress versus strain at break obtained from uniaxial straining experiments at different rates and temperatures. Bills and coworkers³ developed the cumulative damage theory, which describes the failure behavior of solid propellants by a time-to-failure (t_f) under given stress conditions. The stress conditions are defined by the difference between the applied true stress (σ_t) and a critical stress (σ_{cr}) below which no failures are observed. The time-to-failure is a constant for any given stress difference and obeys the Williams-Landel-Ferry (WLF) time-temperature shift law, $(\sigma_t - \sigma_{cr}) = C(\log t_f/a_T)$, where C is a constant and a_T is the WLF shift factor. None of the methods for characterization of failure properties considers mechanical energy dissipations as criteria for microstructural damage.

This paper describes a simple test procedure for measuring the part of the total mechanical energy input which is attributable to the uniaxial damage process from 0% strain to failure. It will be shown that the energy dissipation is a fundamental property of a composite propellant and obeys the WLF time-temperature shift relationship.

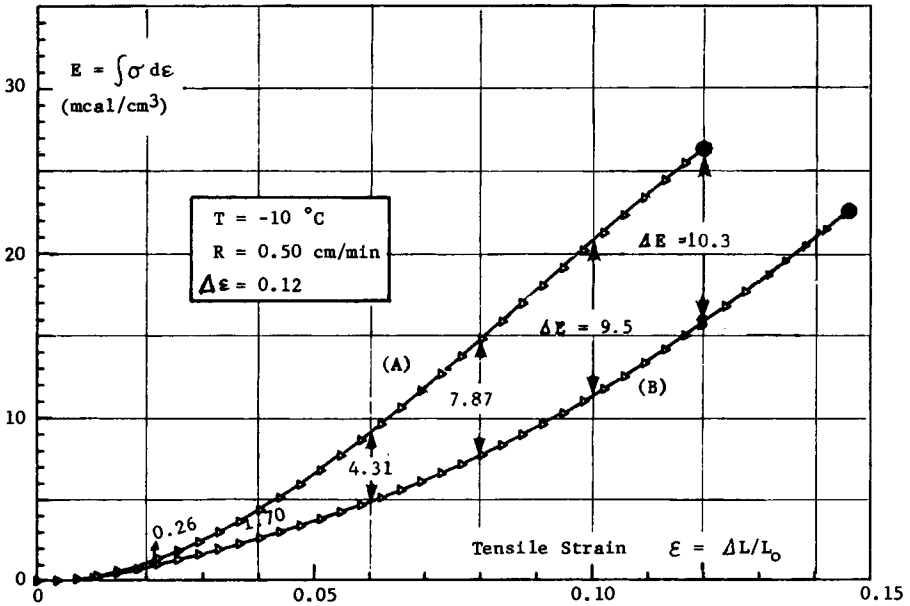
BACKGROUND

The characterization of the strain-dependent damage behavior of a composite propellant by energy balances has been described in previous publications.^{4,5} The term "damage energy" (the amount of energy per unit volume that is attributed to the various damage factors) was introduced to describe the processes occurring during the propellant strain history.

Mechanical energy is required to stretch a tensile specimen from its original length to a given strain. The amount of energy can be determined from the area



(a)



(b)

Fig. 1. (a) Stress-strain test with repeated straining for CTPB propellant. $T = -10^{\circ}\text{C}$, $\dot{\epsilon} = 0.07 \text{ min}^{-1}$, $t_{\text{recovery}} = 60 \text{ min}$ (1 bar = $10^5 \text{ Pa} = 14.5 \text{ psi}$). (A) first stretch, (B) second stretch. (b) Mechanical energy input during repeated straining and determination of damage energy as a function of strain for CTPB propellant (1 mcal = 4.19 J). (c) Damage energy of a CTPB propellant as a function of strain (extrapolation). $T = -10^{\circ}\text{C}$, $\dot{\epsilon} = 0.07 \text{ min}^{-1}$.

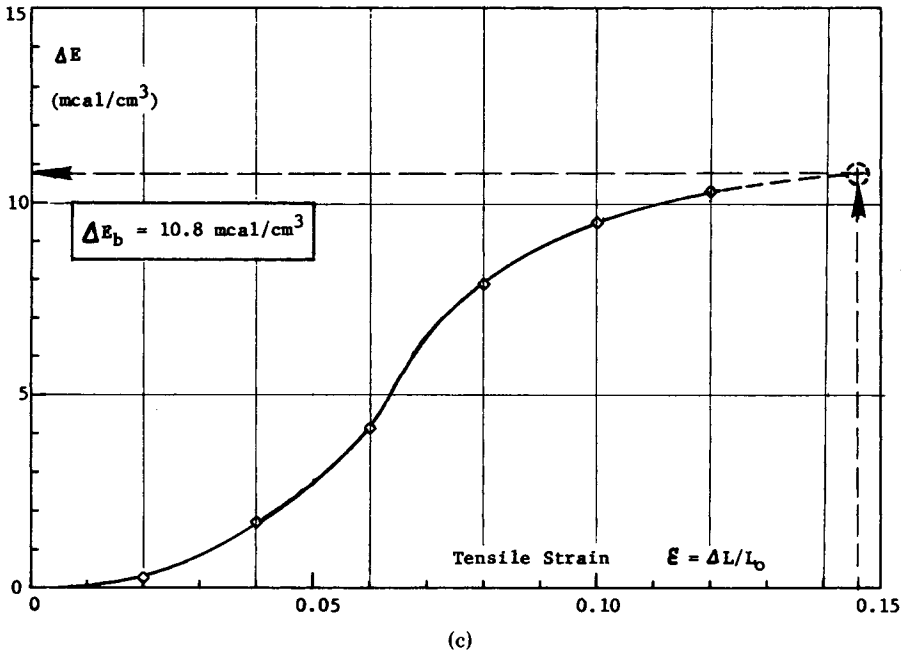


Fig. 1. (Continued from previous page.)

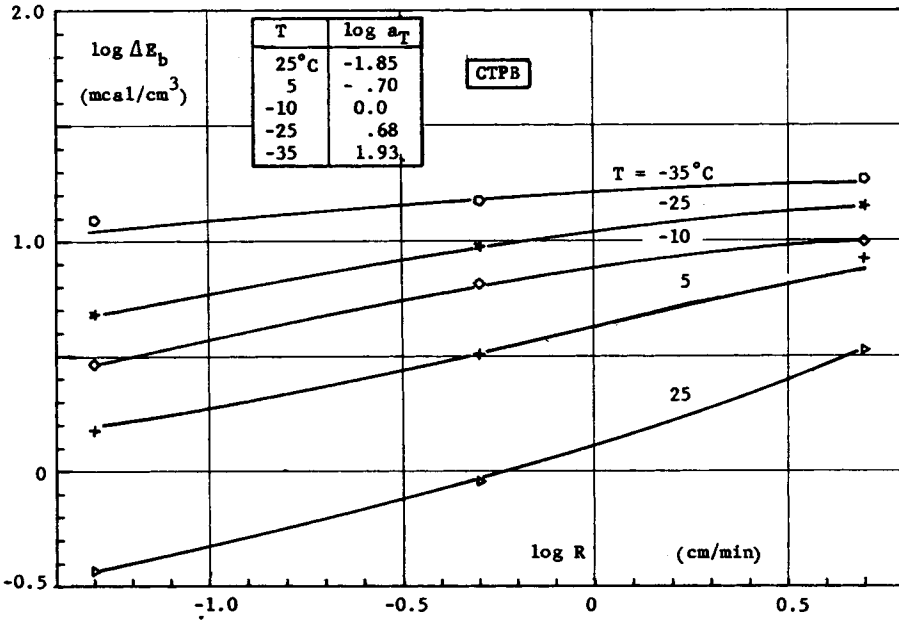


Fig. 2. Total damage energies of a CTPB propellant as a function of temperature and straining rate.

under the stress-strain curve. This energy is dependent on strain rate, strain, and temperature.

Only a part of the energy is actually consumed by the damage that occurs within the propellant structure during a deformation. The other part of the

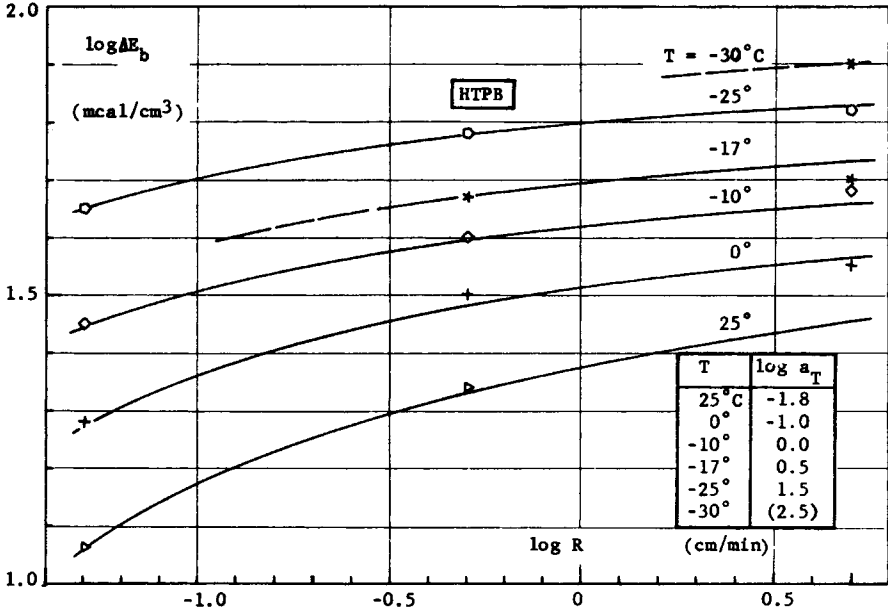


Fig. 3. Total damage energies at failure of HTPB propellant as a function of straining rate and temperature.

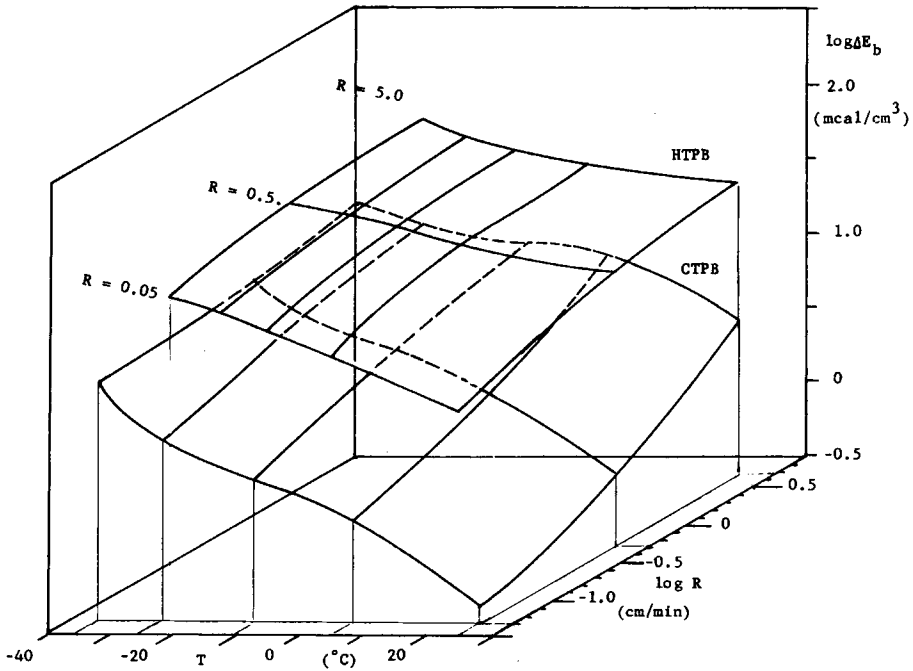


Fig. 4. Total damage energies at failure of CTPB and HTPB propellants as a function of temperature and straining rate.

energy is elastic and is recovered by contractive forces when the specimen is released to its original length. The damage done to a specimen during the first stretch causes a change in physical properties. A second stretch, therefore, re-

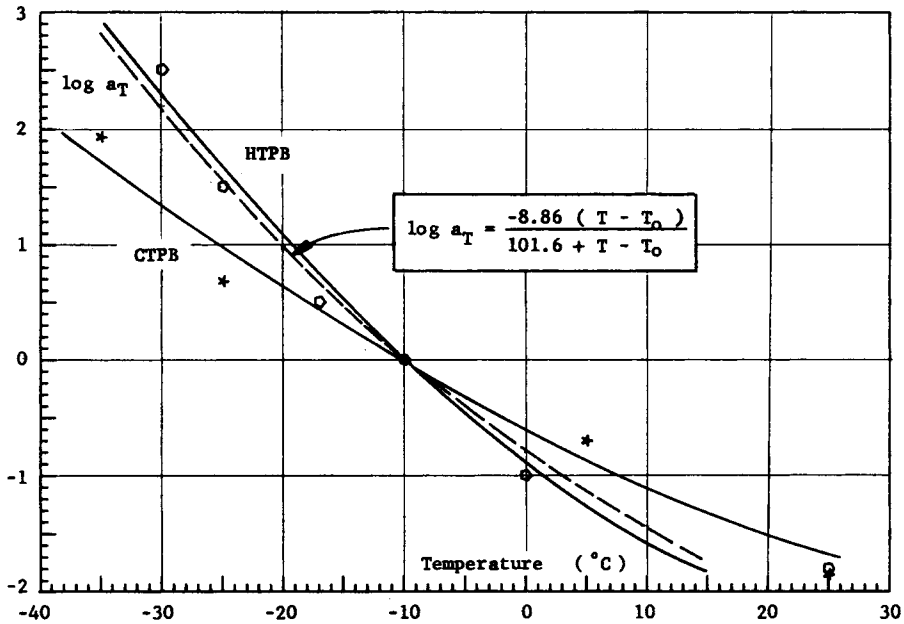


Fig. 5. Time-temperature shift factors for total damage energies of CTPB and HTPB propellants.

sults in a stress-strain path that differs from the first stretch. The area under the second stress-strain curve is always smaller than the area under the first one. The difference in both areas, therefore, represents the energy that dissipated during the damage process along the first stretch. The amount of the dissipated energy is called "damage energy." Theoretical considerations related to the damage energy concept were described earlier.⁵

EXPERIMENTAL

The two propellants used for the test series described here were prepared with a carboxy-terminated polybutadiene (CTPB) and an hydroxy-terminated polybutadiene (HTPB). Both propellants were formulated to contain 14 wt % polymer and 86% solids, consisting of ammonium perchlorate and aluminum metal powder. The CTPB was cured with a tris aziridine curing agent as a part of the polymer system and the HTPB was cured with isophorone diisocyanate as part of the polymer system. In the latter case the HTPB, while having an average functionality near 2, does contain a significant fraction of polyhydroxyl molecules to enable a cure to be obtained with a difunctional comonomer. The ammonium perchlorate consists of a trimodal distribution of particles with an average size of about 50 μ . The aluminum used was about 5 μ in diameter.

The following experimental procedure was used to evaluate the mechanical energy dissipated by the processes discussed. The specimen was stretched to a point just beyond its maximum stress at a given temperature and extension rate in order to induce a damage close to the damage at break. The sample was then driven back to its original length. Some samples were allowed to retract without additional load. Both kinds of samples appeared to recover to the initial

length after 30 min and showed similar restraining curves. The specimen was allowed to recover for 1 hr before it was restrained to failure. A set of typical stress-strain curves (A and B) obtained from such an experiment is presented in Figure 1(a).

The 7-cm-long specimens were epoxy-glued to metal endpieces to avoid any slipping during the test. The samples were machined into a cylindrical shape of 1-cm diameter with conical ends to ensure failure within the uniaxial stress region. Stress-strain curves were recorded via an Instron tester at constant rates from $R = 0.05$ to 5 cm/min ($\dot{\epsilon} \cong 0.007$ – 0.7 min^{-1}) and at five temperatures ranging from 25 to -35°C .

RESULTS

The tensile stresses were computed as engineering or nominal stresses based on the original cross-sectional area of the specimen. Strain values are based on the end-to-end elongation of the sample. The evaluation of the tests is explained in the following example. The area under the stress-strain curves of the first and second stretch in Figure 1(a) is determined by a summation method. The energies obtained are plotted versus strain in Figure 1(b). The energy differences between stretches A and B are indicated in 2%-strain intervals. The ΔE values, or partial damage energies, are plotted in Figure 1(c) as a function of strain. The total damage energy at break ΔE_B is estimated by extrapolation of the partial energies to the failure strain, as indicated by the dashed line.

In this way, the damage energy values at break were determined from similar experiments at various strain rates and temperatures. The results obtained for both CTPB and HTPB propellants are presented in Figures 2 and 3. It appears that the damage energy increases with increasing strain rate and decreasing

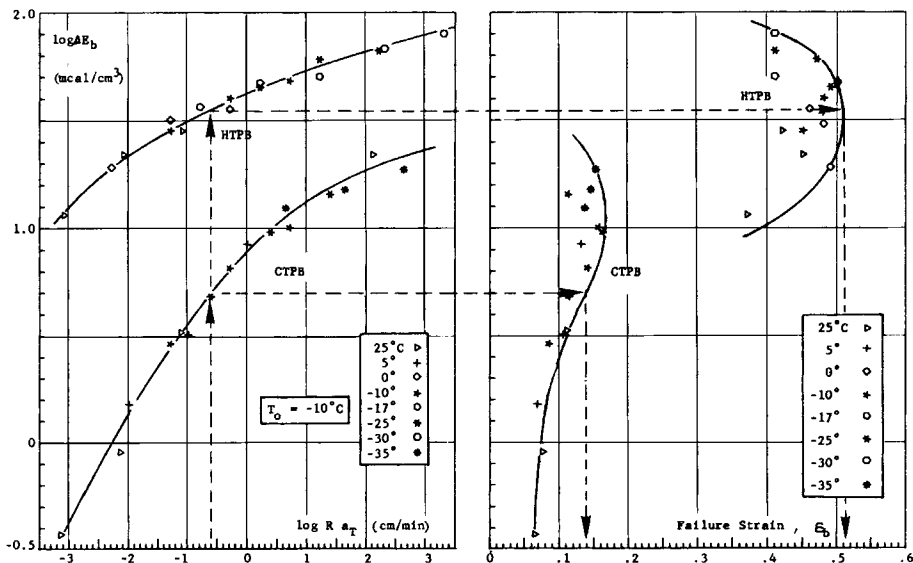


Fig. 6. (a) Reduced master curves for damage energies at break of two propellants. (b) Failure strains versus damage energies of two propellants.

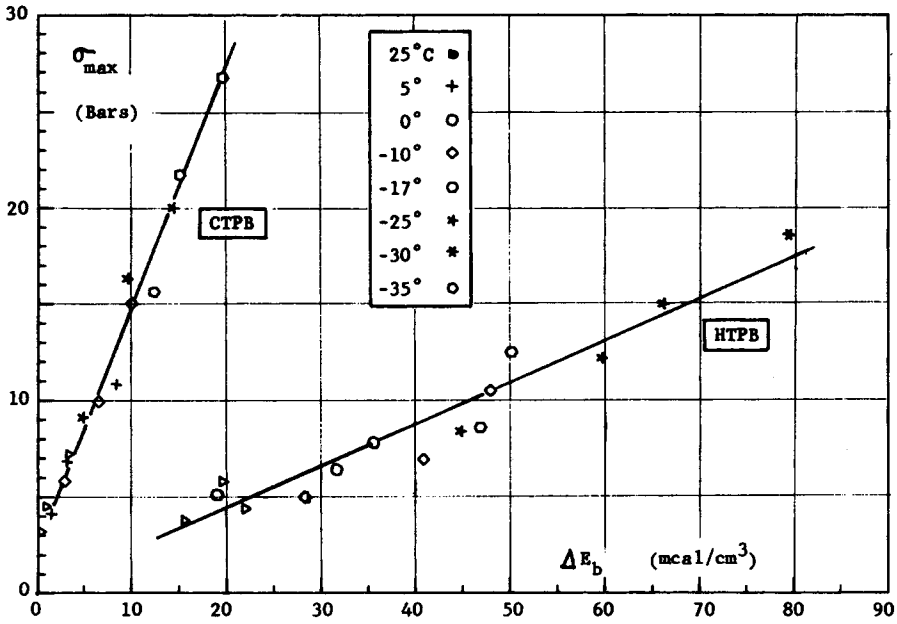


Fig. 7. Maximum tensile stress of the two propellants versus total damage energy at break.

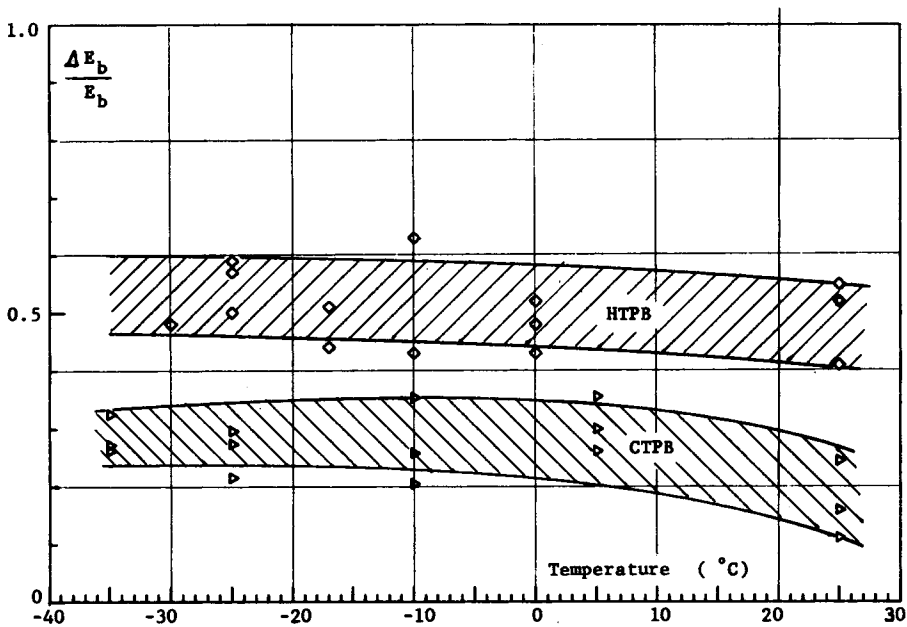


Fig. 8. Fractional damage energy at break as a function of temperature for CTPB and HTPB propellants.

temperature. Shift procedures were applied to the isothermal curves to determine the WLF time-temperature shift factors ($\log a_T$) that are listed in the insert tables in Figures 2 and 3.

A three-dimensional plot of the damage energies of both propellants as a function of temperature and strain rate is shown in Figure 4. The figure shows

two failure surfaces for CTPB and HTPB propellants that can be used as a failure criterion for a given strain rate and temperature test condition. A composite propellant will break when the damage energy under the test conditions reaches its failure surface.

A separate set of WLF shift factors was obtained for each propellant, as indicated in Figure 5. The deviation of the shift-factor curves indicates a different viscoelastic time-temperature behavior of the two propellants.

In presenting the results of this investigation, two alternative methods of examining the data have been used to illustrate how the failure properties of the two propellants can be compared. The curves in Figure 4 show the behavior of the two propellants in a three-dimensional display. A more familiar way of analyzing two propellants is to relate the damage energy master curve to the failure strain envelope, as shown in Figures 6(a and b). The dashed lines demonstrate how the figures can be used to predict ultimate damage energies and failure strains for a given strain rate at a reference temperature. The lower damage energy of the CTPB propellant indicates a smaller extensibility of the propellant structure before failure than HTPB propellant.

The tensile strength of a propellant is not necessarily a criterion for the damage energy value at break. A propellant of high strength can have a lower damage energy at break than a softer propellant. This is demonstrated in Figure 7. The maximum stress of the two propellants, measured at various temperatures, is plotted versus the damage energy at break. The different slopes indicate a different stress-damage relationship for each propellant.

The fractional damage energy at break, defined by the ratio between damage energy and total mechanical energy input until break, describes how much of the mechanical work is actually consumed by the failure process during a straining experiment. The results in Figure 8 indicate that the CTPB propellant uses 15-35% and HTPB propellant 40-60% of the total energy input for the damage process until rupture. The fractional damage energy was found to be primarily dependent on strain rate, with a slight dependence on temperature. The fact that the HTPB propellant uses a larger part of the total energy for damage than the CTPB propellant seems to point to a weaker microstructure of the HTPB propellant. However, it must be considered that the failure strain of the HTPB propellant is approximately 3 times higher than that of the CTPB propellant. A comparison of the fractional damage energies per unit strain, therefore, is a better criterion for the internal resistance of a propellant towards damage and crack formation.

DISCUSSION

It has been shown that the total damage energy at break can be used to characterize the failure properties of propellants as a function of straining rate and temperature. This amount of dissipated energy is actually responsible for the damage and failure and can be divided into two fractions. One part of the damage energy is used for molecular-bond scissions and the other part for disentanglement of polymer chains, dewetting, and viscoelastic losses.

The interfacial contribution, normally called dewetting, can be estimated from normal values of apparent works of adhesion measured at this laboratory from contact-angle measurements and reported previously.⁸ These measurements

TABLE I
Estimation of Broken Bonds in CTPB and HTPB Propellants

Bond	Bond Energies ^a		ΔE_b (mcal/cm ³)		Number of Broken Chains	
	kcal/mol	mcal/bond	HTPB	CTPB	$\delta = 0.1$ HTPB	$\delta = 0.1$ CTPB
C—C	82.6	1.37×10^{-16}	80	20	5.26×10^{17}	1.31×10^{17}
C—O	86.0	1.43×10^{-16}	80	20	5.03×10^{17}	1.26×10^{17}
C—N	72.8	1.21×10^{-16}	80	20	5.95×10^{17}	1.49×10^{17}

^a From Ref. 7.

were made on cleaved single-crystal ammonium perchlorate and optical-quality synthetic sapphire, and values of the order of 80 ergs/cm² were determined. On the average, surface areas of between 1200 and 400 cm²/cm³ of propellant can be calculated (86 wt % solids). Based on these values, the importance of the dewetting contribution can be estimated to be somewhere between 2 and 8 mcals/cm³ if the dewetting were complete (all around the sphere). Since the microscopically observed dewetting is only partial, it has been proposed by the authors that the interfacial separation can account for only a small part of the measured damage energy.

It is assumed that the main part of the accumulated damage energy at break (ΔE_b) was used in the rupture of molecular bonds and only a small fraction (δ) for other damage processes such as disentanglement and dewetting. The number of broken chains (n) per cm³ of propellant can be roughly estimated by the following expression:

$$n = \frac{\Delta E_b \times A}{E_{C-C}} (1 - \delta) \quad (\text{bonds/cm}^3)$$

where E_{C-C} is the chemical bond energy in kcal/mol and $A = 6.022 \times 10^{23}$ is Avogadro's number.

An estimate of the number of broken chains for both propellants at rupture, assuming $\delta = 0.1$ and three different kinds of bonds, C—C, C—N, C—O, is shown in Table I.

Computations reveal that even if 50% of the damage energy ΔE_b is consumed by processes other than bond scissions, the number of broken chains still remains in the region of 10^{17} .

The temperature dependence of the damage energies suggests that the number of broken chains at failure increases at lower temperatures. This is caused by the viscosity increase and consequent changes in the relaxation times. The temperature decrease, which has an effect on the damage energy similar to an increase in straining rate, is described by the WLF shift relationship.

D. M. Pearl carried out the Instron test runs on the CTPB propellant and assisted with the data reduction. Helpful discussions with K. H. Bischel and A. San Miguel during this work are appreciated.

References

1. T. L. Smith, *J. Polym. Sci., Part A*, **1**, 3597 (1963).
2. T. L. Smith, *J. Appl. Phys.*, **35**, 27-36 (1964).
3. K. W. Bills, Jr. and J. H. Wiegand, *Application of an Integrated Structural Analysis to the Prediction of Reliability*. (Ninth Reliability and Maintainability Conference, Detroit, Michigan, 1970) Society of Automotive Engineers, New York, 1970.

4. A. H. Lepie and A. Adicoff, *J. Appl. Polym. Sci.*, **18**, 2165-2176 (1974).
5. A. H. Lepie and A. Adicoff, in *JANNAF Operational Serviceability and Structures and Mechanical Behavior Working Groups, Combined Annual Meeting*, CPIA Publication 253, The Johns Hopkins University, Silver Spring, Md., July 1974, pp. 371-384.
6. M. L. Williams, R. F. Landel, and J. D. Ferry, *J. Am. Chem. Soc.*, **77**, 3701-3707 (1955).
7. T. L. Cottrell, *The Strengths of Chemical Bonds*, Academic, New York, 1958.
8. A. Adicoff and W. E. Stump, in *Third Western Regional Meeting, ACS, Anaheim, California, 30 Oct.-1 Nov. 1967*.

Received January 10, 1978

Revised June 13, 1978